

UKAEA-CCFE-PR(22)34

Ruth Sanderson, Allan Sanderson, Kwame Akowua

# **Development of Digital Tools to Enable Remote Ultrasonic Inspection of Fusion Reactor In-Vessel Components**

Enquiries about copyright and reproduction should in the first instance be addressed to the UKAEA Publications Officer, Culham Science Centre, Building K1/O/83 Abingdon, Oxfordshire, OX14 3DB, UK. The United Kingdom Atomic Energy Authority is the copyright holder.

The contents of this document and all other UKAEA Preprints, Reports and Conference Papers are available to view online free at [scientific-publications.ukaea.uk/](https://scientific-publications.ukaea.uk/)

# **Development of Digital Tools to Enable Remote Ultrasonic Inspection of Fusion Reactor In- Vessel Components**

Ruth Sanderson, Allan Sanderson, Kwame Akowua



# Development of Digital Tools to Enable Remote Ultrasonic Inspection of Fusion Reactor In-Vessel Components

Ruth Sanderson<sup>a\*</sup>, Allan Sanderson<sup>a</sup> and Kwame Akowua<sup>b</sup>

<sup>a</sup>Full Matrix Ltd  
27 Harcombe Road, Cambridge, CB1 9PD, UK

<sup>b</sup>United Kingdom Atomic Energy Authority, Culham Centre for Fusion Energy, Culham Science Centre, Abingdon, Oxon, OX14 3DB, UK.

\* Corresponding author  
07928 440031  
ruth.sanderson@fullmatrix.co.uk

## Abstract

The feasibility of a new approach for pipe inspection has been explored using digital twins to enhance guided wave inspection. Guided wave inspection is well-established in the oil and gas industry to screen remotely long lengths of predominately straight pipeline for corrosion. However, inspection of complex geometries of pipe remains a challenge. Nuclear fusion facilities are one such potential application. Fusion reactors will have a network of many kilometres of service pipes with complex features including multiple pipe bends. Some of these pipes could be use for actively cooling components such as the First Wall and Divertor.

Guided ultrasonic wave inspection has the significant advantage of offering 100% coverage of the pipe wall over tens of metres of pipe from a remote test location. This is highly attractive, particularly in the nuclear industry where it is important that human presence in high risk areas is prohibited due to high radiation doses and temperatures. In this work, finite element wave propagation models have been investigated as digital twins of fusion reactor components. The models have been used to calculate bespoke excitation signals that will allow full volumetric inspections of these complex pipes to be carried out from a remote location.

For the first time, it has been demonstrated that models can be used to successfully correct for the distortion caused by multiple pipe bends. This has resulted in an improvement to detection capability by an order of magnitude over a conventional guided wave set-up. The digital twin technique developed here therefore shows significant promise for future inspection of nuclear fusion power plant pipes.

## 1. Introduction

Guided wave inspection was commercialised in the late 1990s [1-3]. Screening procedures for corrosion detection in pipelines were developed using axisymmetric wave modes excited and received with rings of piezoelectric transducers. A patch of corrosion of at least 5% of the cross section can be detected, and the axial distance of the defect

from the tool location is provided along with an estimate of cross sectional area (CSA) loss. Shortly after commercialisation, the advance of computer hardware and software meant that commercial finite element packages could be used to simulate large three-dimensional guided wave problems and provide a useful insight into the physical phenomena [4-6].

Guided wave inspection is most commonly used for screening of petrochemical pipeline. It has the significant advantage over alternative techniques of full volume inspection of tens of metres from a single test location [7-9] and only requires a relatively small region of access. This means that it is particularly valuable in scenarios where the pipe to be inspected is inaccessible. The technique is now maturing in straight pipeline and is advancing from a screening only procedure to being able to provide information on flaw size and shape [10-17]. However, for wider applications, there are many features that could be present such as pipe bends, pipe branches, pipe supports, flanges or even other flaws. The presence of these features adds complexity to the received signals making quantitative interpretation of the inspection results problematic.

The supply pipes in fusion reactors are one such example where multiple bends as well as other features such as bellows and pipe branches are included in the design. Figure 1 shows a schematic of the ITER divertor supply pipes [18]. There is a region where manual access might be possible; a potential site for a guided wave tool and then regions where access is restricted or impossible. Remote inspection of these regions would be highly valuable.

In the work presented here, finite element analysis has been used to simulate wave propagation in an example provided by ITER of divertor supply pipes with a view to creating a digital twin. This was used to both compute bespoke excitation signals to apply, and to interpret received signals in order to correct for the distortion caused by the presence of multiple pipe bends. This has improved detection capability in complex pipe geometries and paved the way for quantitative assessment of flaws to be carried out.

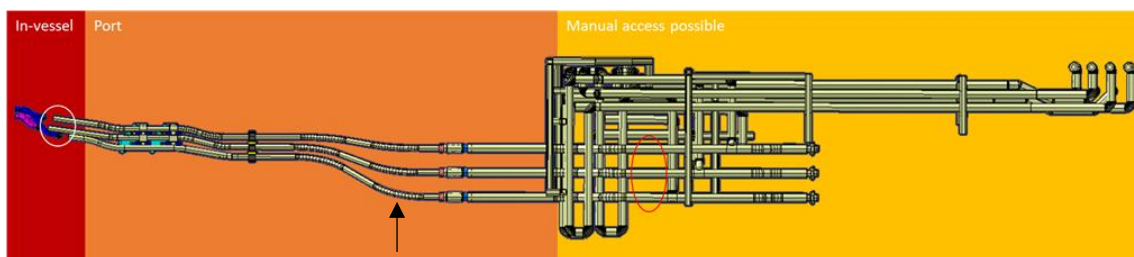


**Figure 1. Overview of divertor pipes. The red circle indicates where the inspection equipment could be situated, the white circle indicates the region of interest for inspection and the arrow indicates the pipe that was selected for this study.**

## 2. Approach

### 2.1 Geometry and material properties

Full three-dimensional models were generated of the ITER divertor pipe. The divertor supply pipes are complex with multiple bends, transition sections, welds, pipe supports, flanges, branches and a bellows feature. The majority of the pipe was assumed to be 2.5” Schedule 10 (73mm outer diameter and 3.05mm wall thickness) 316L austenitic stainless steel.

The pipe supports were assumed to have sufficient insulation to prevent transmission of acoustic waves so were not included in the simulation. The pipe branches, welds, flanges and transition sections were included in the models. A bellows feature was present in the ITER design to allow for expansion and contraction of the pipe due to temperature variations. The bellows were found to strongly affect the signals and may not be present in future applications of the technology, so it was omitted from the full-scale models for the purposes of this study.

Figure 2 shows the resulting full-scale model. It contained a total of eight bends varying from 6 degrees to 45 degrees, all with a 1000mm bend radius. This was a significant increase in complexity compared with the previous state-of-the-art of a demonstration of distortion correction for a single journey through one 90-degree bend [19].

In order to simulate the ongoing pipe, absorbing boundary conditions (or infinite elements) were used on all of the free ends. The branch pipe was included in the model since this is a large reflector and it is important to establish whether it will cause issues with the inspection technique.

The divertor pipe was assumed to be made of 316L stainless steel with the following material properties:

Young’s modulus = 200GPa

Poisson’s ratio = 0.27

Density = 7990.0 kg/m<sup>3</sup>

The commercially available software, ABAQUS version 2020 was used to generate, solve and post process all of the models.

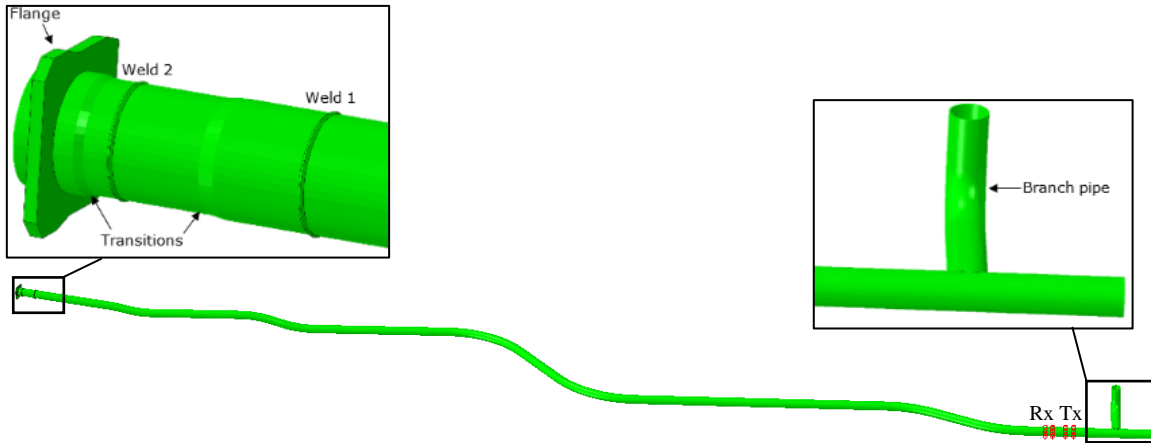


**Figure 2. Full-scale finite element model generated of one of the ITER divertor pipes.**

## ***2.2 Loads and boundary conditions***

In all cases, rings of transducers were simulated as eight point sources around the circumference of the pipe. Point source excitation has been found to be a sufficiently accurate representation in past work [14,20,21]. The transducer rings were positioned approximately 9m from the region of interest. Loads were applied in the torsional direction.

Four rings of transducers were simulated: two receiver rings and two transmitter rings. The pairs of rings were used to control the direction of the waves on reception and transmission respectively. With a pair of rings, there are two main options for the ring cancellation algorithm: either optimising for ‘backwards suppression’ or ‘forwards enhancement’. Backwards suppression ensures that no waves travel in the backwards direction but will affect the shape of the forwards propagating signal. Conversely, enhancing the forwards propagating signal will cause transmission of an ideal waveform in the forwards direction, at the expense of an imperfect backwards cancellation of the waves. Both options were investigated in combination with the digital twin distortion correction technique.

Absorbing boundary conditions were applied on the free ends of the model to efficiently simulate the continuation of the pipe. This was achieved using ‘infinite elements’ in Abaqus.

Other than the loads and absorbing boundary described above, no other loads or boundary conditions were applied to the model; it was assumed that the pipe was in a free state. It was also assumed that the sound waves were not attenuated by any materials in contact with the pipe. Amplitude losses in the signal arising from dispersion, mode conversion and reflection/transmission or interference effects were simulated by the model.



### ***2.3 Finite element mesh***

A meshing strategy of eight elements per minimum possible wavelength was adopted that has been used and experimentally validated by many previous authors [3-6]. In order to be conservative, this was calculated for the highest frequency pulse used in this study (14-cycle 28kHz). In a 2.5" Schedule 10 stainless steel pipe for this excitation, an eighth of the minimum possible wavelength was around 4mm. Elements of this size were therefore used along the length and around the circumference. In all cases, 4 elements were used through the thickness. Three-dimensional brick elements with reduced integration were used. The time step size used was 0.1 $\mu$ s for all the cases in order to satisfy the stability limit for the analysis.

### ***2.4 Distortion correction technique***

The distortion correction technique was previously developed and successfully tested on a single 90 degree, 229mm mean radius pipe bend in a 3-inch Schedule 40 (88.9mm outer diameter, 5.49mm wall thickness) steel pipe with a 10-cycle 25kHz excitation [19, 20]. The method is summarised here as follows:

1. Firstly, an excitation of the desired pulse is generated in the region of interest. For example, the fundamental torsional mode, T(0,1) in isolation.
2. The signal received at the intended transducer ring location is then filtered using a spatial filtering technique to separate out the wave modes [13].
3. The signals are then time-reversed.
4. Finally, the signals are recombined with scaling factors applied to take account of the relative excitability of each of the wave modes. These were calculated using previously developed methods [21].

### ***2.5 Processing of signals from flaws to remove signal distortion with the digital twin***

In general, guided wave inspection is capable of detecting changes in acoustic impedance such as a change in cross sectional area caused by corrosion, for example. In order to understand the detection capability for these types of flaws, seven different postulated flaws in a weld were simulated in the full-scale model. The dimensions of the cracks studied were based on defect geometries provided by the UK Atomic Energy Authority (UKAEA). In addition, some corrosion flaws were included in the study. All of the flaws studied were part-wall and part-circumference. Figures 3 and 4 show the geometry of the different flaws studied.

The flaws were assumed to be at weld 2 (Figure 2).

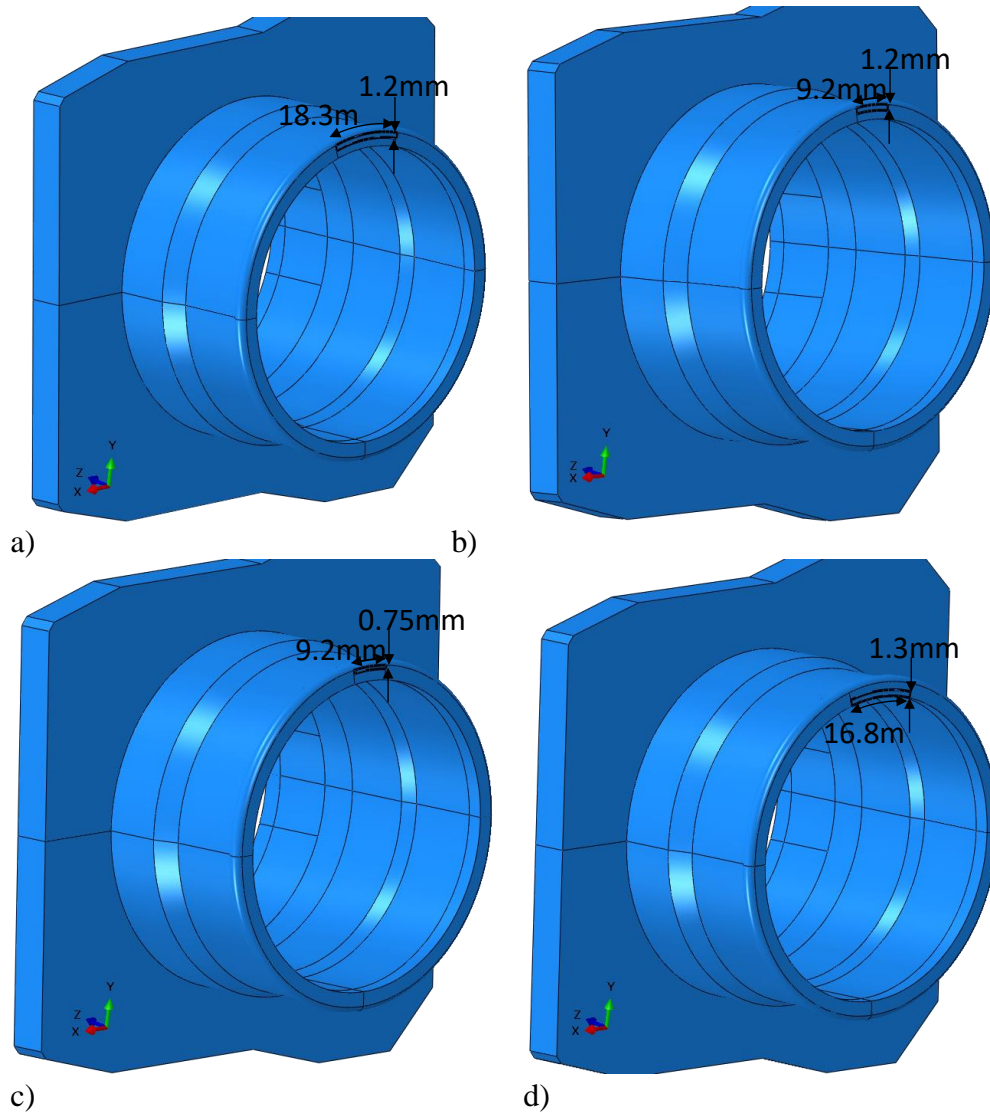


**Figure 3 Geometry of cracks (shown in bold outline) studied. Note: the main pipe has been cut away to show the crack inside:**

- a) 3.5% cross sectional area loss external crack;**
- b) 2.4% cross sectional area loss external crack;**
- c) 1.1% cross sectional area loss external crack;**
- d) 3.5% cross sectional area loss internal crack.**

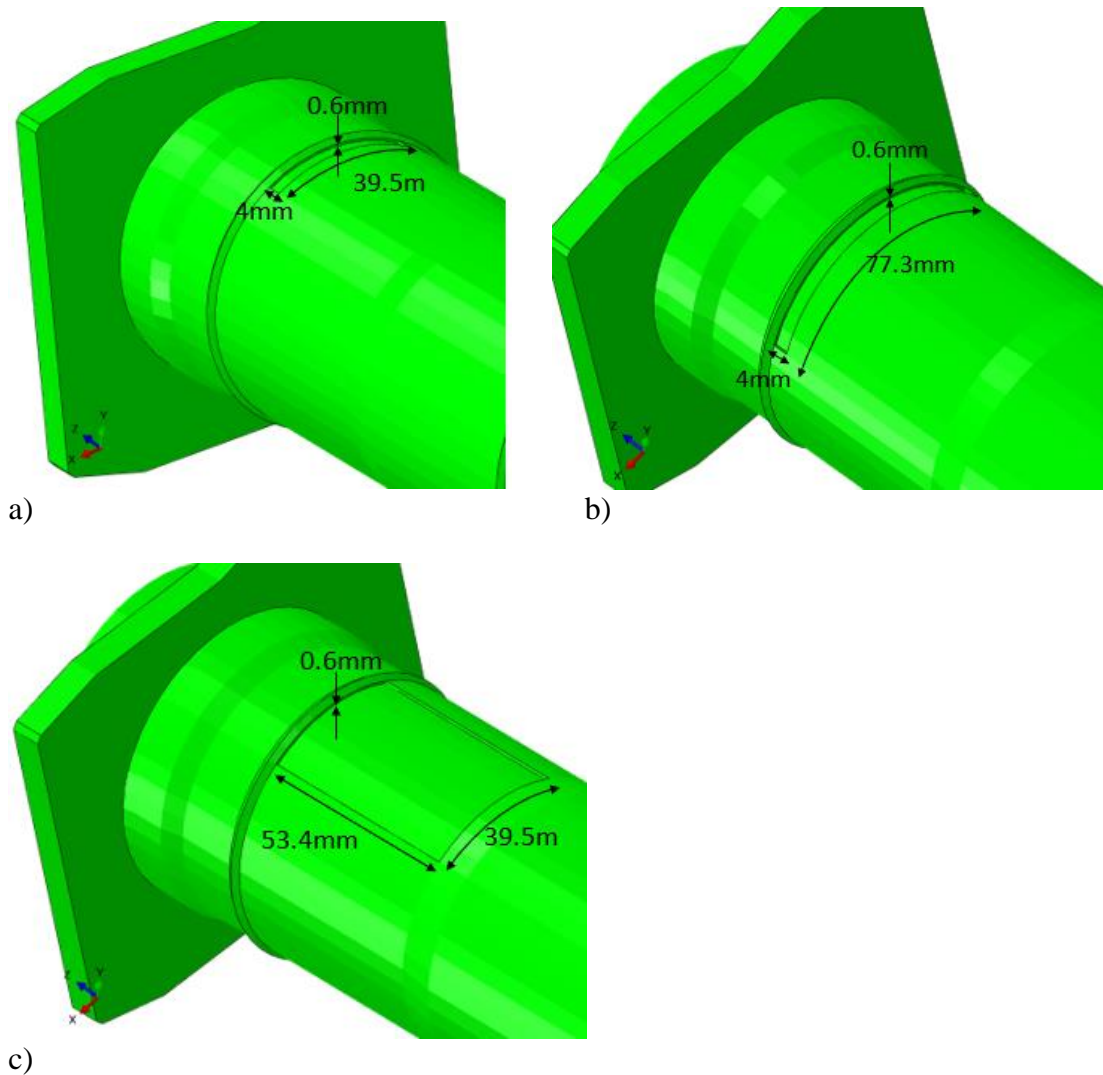


**Figure 4 Geometry of corrosion studied:**  
**a) 4% cross sectional area loss external corrosion;**  
**b) 7.4% cross sectional area loss external corrosion;**  
**c) 4% cross sectional area loss internal corrosion (axially long).**

In straight pipe, it is possible to detect flaws in a newly made weld by examining the flexural content of the reflection. Since welds are axisymmetric, flexural reflections will only occur if a flaw is present. However, the asymmetry of the flange in the ITER divertor supply pipe scenario studied here also adds flexural wave modes to the signal, and to a much greater extent than expected contributions from a small crack. Therefore, this method is only likely to work for large flaws such as extensive corrosion.

It is possible to overcome these problems by using a baseline subtraction technique. This is where a flaw-free baseline signal is collected, and subsequent signals are compared to this to monitor the condition of the pipe. A baseline subtraction technique cannot be used for situations such as a newly made weld. However, it is likely to be more practical to

inspect a new weld using an alternative NDT technique as part of the remote welding device at the time of manufacture anyway.

Therefore, the signals were processed by first carrying out a baseline subtraction from an otherwise identical flaw free model. The baseline subtracted signals were then time-reversed and applied to the digital twin model with the elongated ends used to calculate the excitation signals. Then, the same process of mode filtering, time reversal and recombination with scaling factors for excitability was then applied, except this time with receivers at the location of interest instead. This resulted in a computation of the reflection from flaws in the interest of location as if the pipe bends had not been present.

### **3. Results and Discussion**

#### ***3.1 Calculation of bespoke excitation signals with the digital twin***

Before attempting to predict detection capability for a range of flaws, the effectiveness of the distortion correction technique for generating the desired signals at the location of interest was tested. This was achieved using a modified version of the full-scale model with just the eight bends and with elongated straight sections of pipe added to the ends. This allowed the resulting signals to be examined without any reflections or interactions with features occurring.

Three different options were tested as follows:

- a 5-cycle 10kHz pulse to be achieved beyond the bends
- a 14-cycle 28kHz pulse to be achieved beyond the bends
- A focus at 10kHz at a single circumferential location

Figures 5 and 6 show the results of applying the bespoke excitations to the modified full-scale model compared with the relevant conventional guided wave excitations of Hann windowed pulses (5-cycle 10kHz and 14-cycle 28kHz). Figure 5 also includes a comparison of different ring spacings and cancellation algorithms used.

It can be seen that the bespoke signals are highly effective in correcting for the signal distortion caused by the bends. The axial symmetry of the signal and lack of spurious flexural ‘noise’ is evident particularly in Figure 5c where forward enhancement has been simulated with the two rings. There is some residual noise observed in the distortion corrected 5-cycle 10kHz example (Figure 5b). This is caused by imperfect ring cancellation, most likely a combination of a sub-optimal ring spacing and the effect of backwards cancellation on the forwards propagating signal.

The 28kHz full-scale models were carried out with backwards suppression and the rings spacing was altered to be optimal for this frequency to allow a fair comparison of the capability at 28kHz to be made. It can be seen that the backwards suppression algorithm works well and there is no discernible noise present (Figure 6b) compared with the equivalent conventional excitation of 14-cycle 28kHz where flexural ‘noise’ is observed.

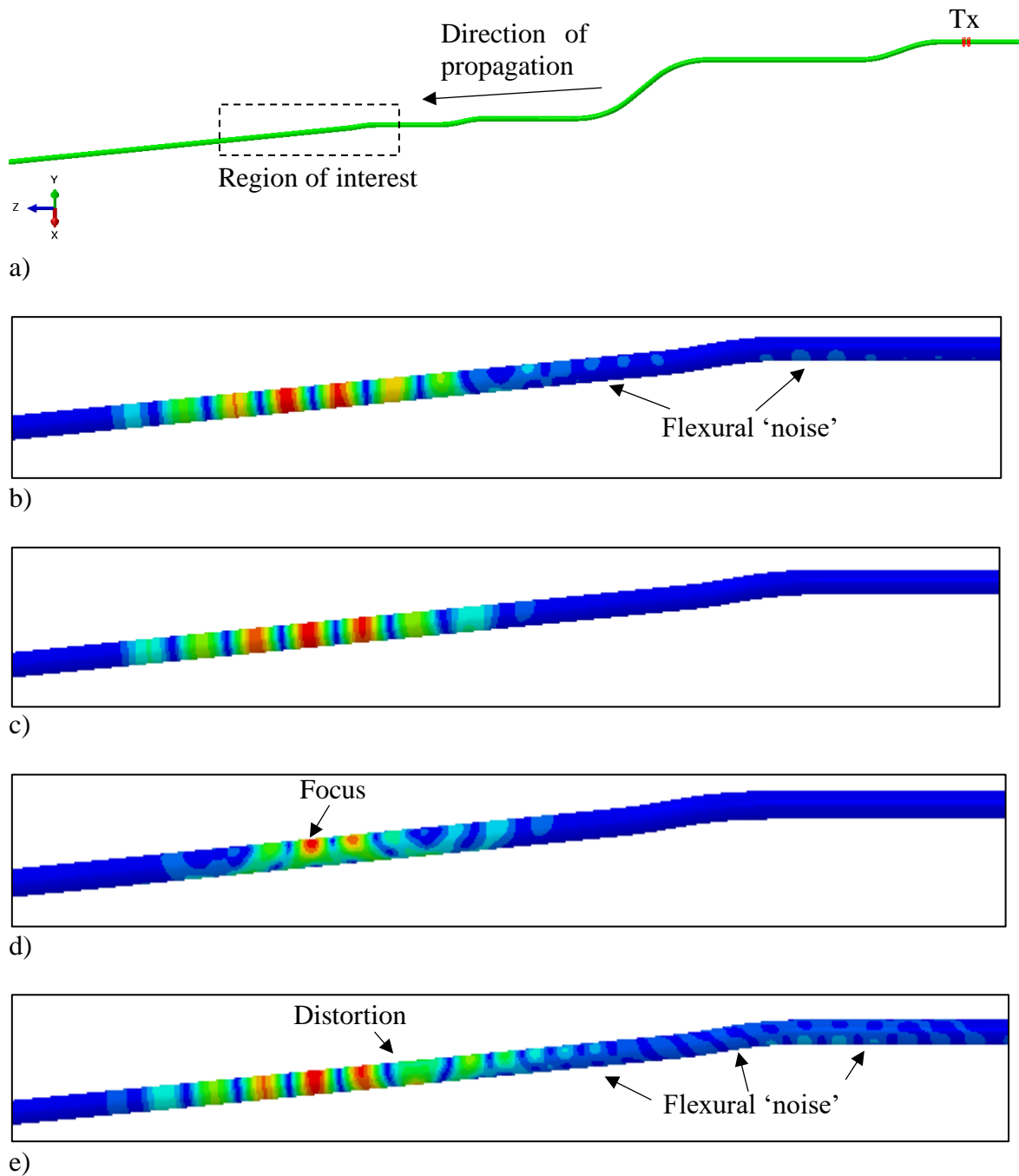


**Figure 5. Von-Mises stress plots showing the guided wave pulse after propagating through the bends to illustrate the effectiveness of the distortion correction technique at 10kHz:**

- a) Overview of the full-scale distortion correction demonstration model;
- b) Distortion corrected 5-cycle 10kHz with backward ring suppression and 62mm spacing (model ref. e75). The main signal is axisymmetric as desired but some flexural wave modes are observed behind, contributing to noise;
- c) Distortion corrected 5-cycle 10kHz with optimal ring spacing of 79mm and forwards ring enhancement. The main pulse is axisymmetric with no obvious noise;

- d) Distortion corrected 10kHz focusing with backward ring suppression and 62mm spacing. A peak amplitude is observed at one location in the pipe;
- e) Conventional 5-cycle 10kHz excitation. The main pulse is not axisymmetric and flexural wave modes are observed behind, contributing to noise.

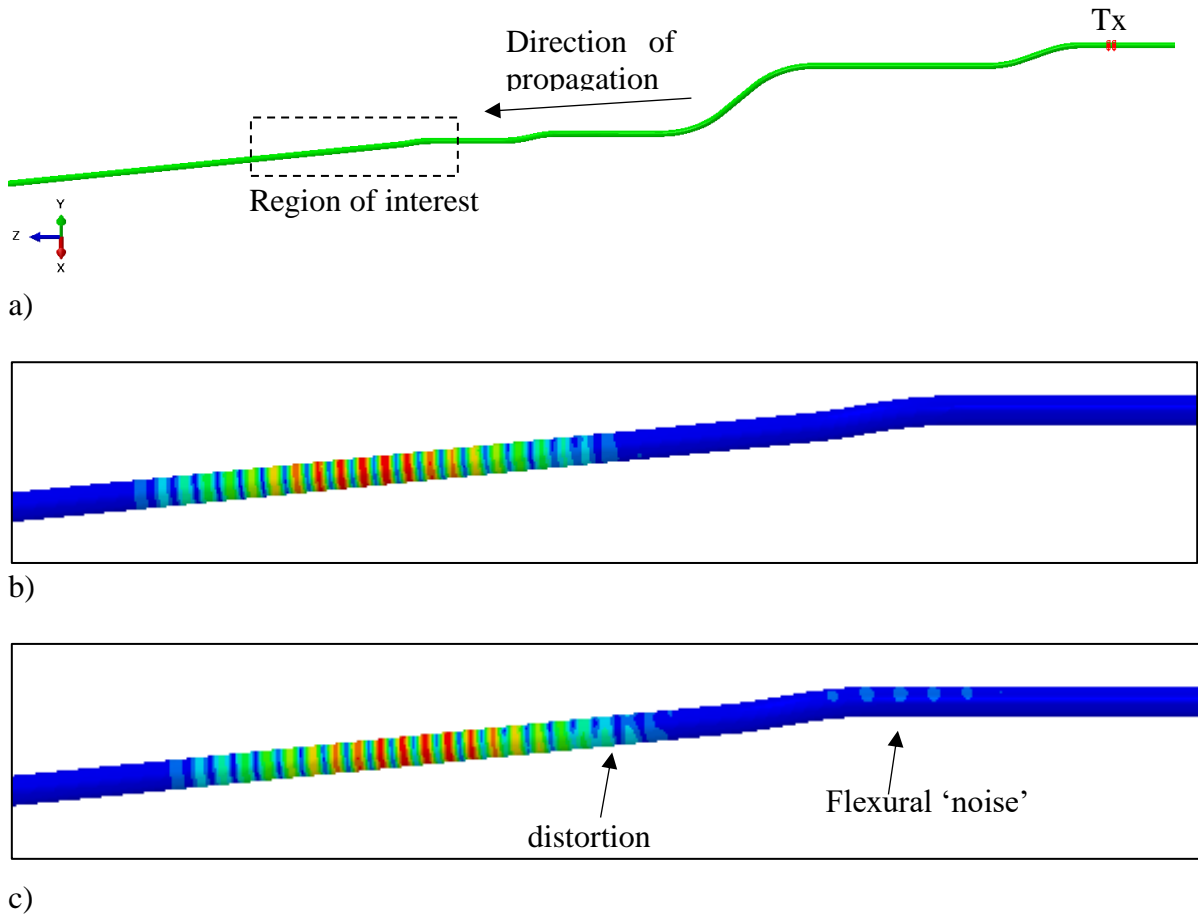


**Figure 6. Von-Mises stress plots showing the guided wave pulse after propagating through the bends to illustrate the effectiveness of the distortion correction technique at 28kHz:**

- a) Overview of the full-scale distortion correction demonstration model;
- b) Distortion corrected 14-cycle 28kHz signal (model ref. e77) with backwards suppression used. The main pulse is axisymmetric with no obvious noise;
- c) Conventional 14-cycle 28kHz excitation (model ref. e79) The main pulse has some distortion and there some flexural wave modes are observed behind it which will contribute to noise.

Figure 7 shows a polar plot of the focus spot achieved at 10kHz. The spot is relatively wide which would be expected due to the low number of existing modes at a frequency of 10kHz. The maximum amplitude occurs at the intended circumferential location of 270 degrees and is low elsewhere with only a small lobe on the opposing side (a commonly observed feature with guided wave focusing). The fact that a highly uniform focus is achieved at the desired location beyond the eight bends, demonstrates that the digital twin

concept of using a model to calculate bespoke excitation signals, removing distortion caused by pipe bends is effective.

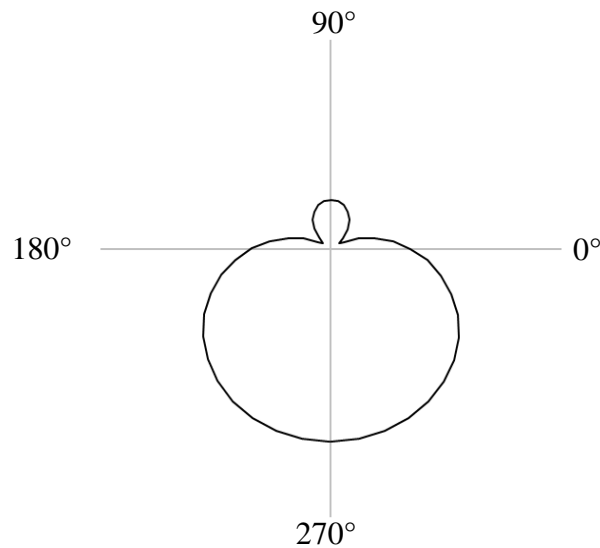


**Figure 7. Polar plot of the focus achieved in the distortion corrected focus model at 10kHz (model ref. e76). The amplitude can be seen to be largest at the intended 270-degree location indicating that focusing can be achieved using the digital twin.**

### ***3.2 Prediction of detection capability using the digital twin distortion correction technique***

Detection capability of any NDT technique is determined by the level of signal compared to the level of noise. As such, in order to predict detection capability from the full-scale modelling results, it was necessary to assume a representative level of noise in the repeatability of experimental data i.e., the difference between two theoretically identical experimental measurements relative to the amplitude of the incident wave mode. A value of 0.1% or -60dB was assumed for the purposes of this study.

Table 1 gives details of the models and the reflection coefficients predicted by the model for each using the distortion correction method. In order to detect a flaw using the method, the reflection from the flaw would need to be at least twice that of the residual noise after baseline subtraction in the experiment, therefore flaws with predicted reflection coefficients of -54dB or higher would be detectable.

This means that both the external and internal 3.5% CSA loss cracks, and all the corrosion is detectable using the distortion correction technique. For an equivalent Hann window guided waves excitation without distortion correction, the external 3.5% CSA loss crack was predicted to have a reflection coefficient of 0.075% or -62.5dB. This would therefore not be detectable. Moreover, there is a 4.4 times improvement in signal to noise arising from the use of the distortion correction technique.

**Table 1 Predicted reflection coefficients at 10kHz using the distortion correction technique**

Model ref.	Flaw description (through-wall extent x circumferential extent x axial extent)	Reflection coefficient, %
e46	1.2mm x 18.3mm external crack (3.5% CSA loss)	0.330 (-49.6dB)
e47	1.2mm x 9.2mm external crack (2.4% CSA loss)	0.126 (-58.0dB)
e48	0.75mm x 9.2mm external crack (1.1% CSA loss)	0.058 (-64.7dB)
e51	1.3mm x 16.8mm internal crack (3.5% CSA loss)	0.201 (-53.9dB)
e64	0.6mm x 39.5mm x 4.0mm external corrosion (4% CSA loss)	1.224 (-38.2dB)
e65	0.6mm x 77.3mm x 4.0mm external corrosion (7.4% CSA loss)	2.432 (-32.3dB)
e66	0.6mm x 39.5mm x 53.4mm external corrosion (4% CSA loss)	5.071 (-25.9dB)

At 28kHz the predicted reflection coefficient for the 3.5% cross sectional area loss crack was -58dB compared with -63.1dB for a Hann window pulse (14-cycle 28kHz). Although the distortion correction technique increases the reflection coefficient by a factor of 1.8, this is not enough to make it detectable at this frequency. The reduction in improvement observed is thought to be the result of the lack of flexural wave mode activity at this frequency.

Finally, the reflection coefficient for the 10kHz distortion corrected focus condition was predicted to be 0.74% or -42.6dB. This is a factor of 10 improvement on the detection capability of a conventional 5-cycle 10kHz excitation. This crack would therefore be easily detectable using the distortion corrected focus condition for the assumed experimental repeatability noise level of -60dB.

Finite element analysis has been used here in the first instance to test and examine the distortion correction techniques and assess the feasibility of a digital twin. In future, the analytical modelling techniques previously developed [19-21] could be used to make it possible to use the digital twin in real-time. The digital twin could also potentially be updated depending on the condition of the pipe and changes to the environment.

#### **4. Conclusions**

The feasibility of developing a digital twin for remote monitoring of nuclear fusion supply pipe has been investigated. Finite element analyses have been used to calculate bespoke signals to apply in order to inspect predetermined regions of the pipe and to reconstruct the distorted signals from flaws after propagating through a number of pipe bends.

The following detailed conclusions are drawn:



1. A full-scale finite element model has been developed based on the pipes in the ITER divertor. The model has been used to predict the detection capability of a range of different cracks and corrosion flaws in different locations.
2. It is possible to use the digital twin to calculate bespoke signals that generate either pure axisymmetric signals or a focus at a desired location beyond multiple bends.
3. The digital twin distortion correction technique has been shown to significantly improve detection capability with an increase of signal to noise by a factor of 4.4 better than using the guided wave system in a conventional way.
4. The focusing concept, using the model as a digital twin, increases the detection capability by increasing signal to noise by a factor of 10, predicting that a 3.5% CSA loss part-wall, part-circumference, crack (or larger) would be easily detectable with equipment capable of a repeatability noise to signal level of -60dB SNR.

In summary, for the first time, a digital twin technique has been developed that can be used to successfully correct for the distortion in guided wave signals caused by multiple pipe bends. The technique is predicted to yield an order of magnitude improvement in detection capability over conventional guided wave inspection. The technique shows significant promise for future inspection of nuclear fusion power plant pipes and other industries such as existing nuclear, petrochemical and food processing.

### **Acknowledgements**

The authors are grateful for the funding for this project received by UKAEA's new 'Fusion Industry Programme' and awarded through the UK Government 'Small Business Research Initiative', Project Number 12679.<sup>1</sup> The authors also acknowledge and greatly value the support of the rest of the UKAEA project team and are grateful to ITER for providing the CAD of the divertor pipe.

### **References**

1. P. Mudge, A. Lank and D. Alleyne, 'A long range method of detection of corrosion under insulation in process pipe work'. In: 5th European Union Hydrocarbons Symposium, Edinburgh, 26-28 November, 1996.
2. M. Lowe, D. Alleyne, and P. Cawley, 'Defect detection in pipes using guided waves.', *Ultrasonics*, 36, pp147-154, 1998.
3. D. Alleyne and M. Lowe, 'The reflection of guided waves from circumferential notches in pipes.', *ASME J Appl Mech*, 65, pp635-641, 1998.
4. F. Moser, L. Jacobs and J. Qu, 'Modeling elastic wave propagation in waveguides with the finite element method.', *NDT&E International*, 32, pp225-234, 1999.
5. R. Sanderson and S. Smith. 'The Application of Finite Element Modelling to Guided Ultrasonic Waves in Rails', *Insight*, 44(6), 2002.
6. R. Sanderson, 'The application of finite element modelling to guided wave testing systems.', *Review of Progress in Quantitative Nondestructive Evaluation*. AIP Conference Proceedings, 2003.

---

<sup>1</sup> The views expressed in this publication are those of the authors and not necessarily those of UKAEA.

7. P.J. Mudge, 'Field application of the Teletest® long-range ultrasonic testing equipment', *Insight*, 43(2), pp74-77, 2001.
8. D.N. Alleyne, B. Pavlakovic, M.J.S. Lowe and P. Cawley, 'Rapid, long range inspection of chemical plant pipework using guided waves', *Insight*, 43(2) pp93-96, 2001.
9. H. Kwun, S. Y. Kim and G. M. Light, 'The Magnetostrictive Sensor Technology for Long Range Guided Wave Testing and Monitoring of Structures' *Materials Evaluation*, pp80-84, 2003.
10. A. Demma, P. Cawley, M. Lowe, A. Roosenbrand and B. Pavlakovic, 'The reflection of guided waves from notches in pipes: a guide for interpreting corrosion measurements.', *NDT&E International*, 37(3), pp167-180, 2004.
11. R. Sanderson, 'Long range ultrasonic guided wave focusing in pipe with application to defect sizing' *ICU Conference*, 2007.
12. P. Catton, P. Mudge and W Balachandran, 'Advances in Defect characterisation using Long Range Ultrasonic Testing of Pipes', *Insight*, 50(9), 2008.
13. P. Catton, 'Long Range Ultrasonic Guided Waves for the Quantitative Inspection of Pipelines.', Ph.D. thesis, Brunel University, 2009.
14. R. Sanderson and P. Catton, 'The reflection of guided waves from multiple flaws in pipes', *J. Nondestruct. Eval.*, 32, pp384-397, 2013.
15. J. Mu, L. Zhang and J. Rose, 'Defect circumferential sizing by using long range ultrasonic guided wave focusing techniques in pipe.', *Nondestructive Testing and Evaluation*, 22(4), pp239-253, 2007.
16. R. Sanderson and P. Catton, 'Flaw sizing in pipes using long-range guided wave testing', *Review of Progress in Quantitative Nondestructive Evaluation*, Volume 30, 2011.
17. R. Carandente, and P. Cawley, 'The effect of complex defect profiles on the reflection of the fundamental torsional mode in pipes.', *NDT&E International*, 46, pp41-47, 2012.
18. J P Friconneau, O David, J P Martins, J D Palmer and A Tesini, 'Assessment of a cooperative maintenance scheme for ITER divertor cooling pipes', *Fusion Engineering and Design*, Volumes 75-79, pp 531-535, November 2005.
19. R. Sanderson, D. Hutchins, D. Billson and P. Mudge: 'The investigation of guided wave propagation around a pipe bend using an analytical modelling approach', *Journal of the Acoustical Society of America*, 133 (3), pp. 1404-1414, March 2013.
20. R. Sanderson: 'Quantitative Studies in Guided Wave Inspection of Pipelines', PhD thesis, University of Warwick, October 2012.
21. R. Sanderson and P. Catton: 'An Analytical Model for Guided Wave Inspection Optimization for Prismatic Structures of Any Cross Section', *IEEE Transactions on Ultrasonics, Ferroelectrics, and Frequency Control*, vol. 58, no. 5, May 2011 pp 1016-1026.